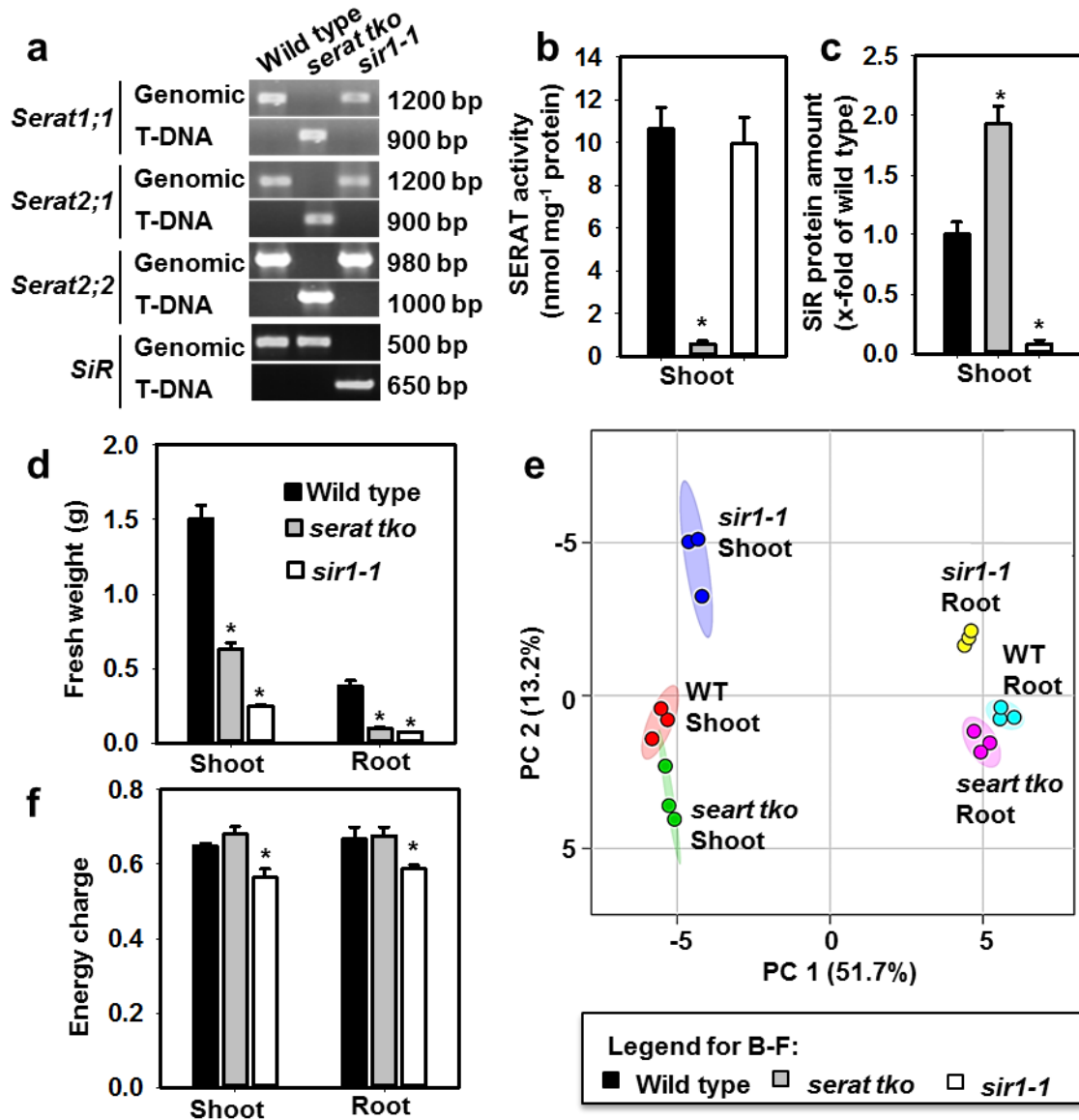


Supplementary Figures:

Supplementary Fig.

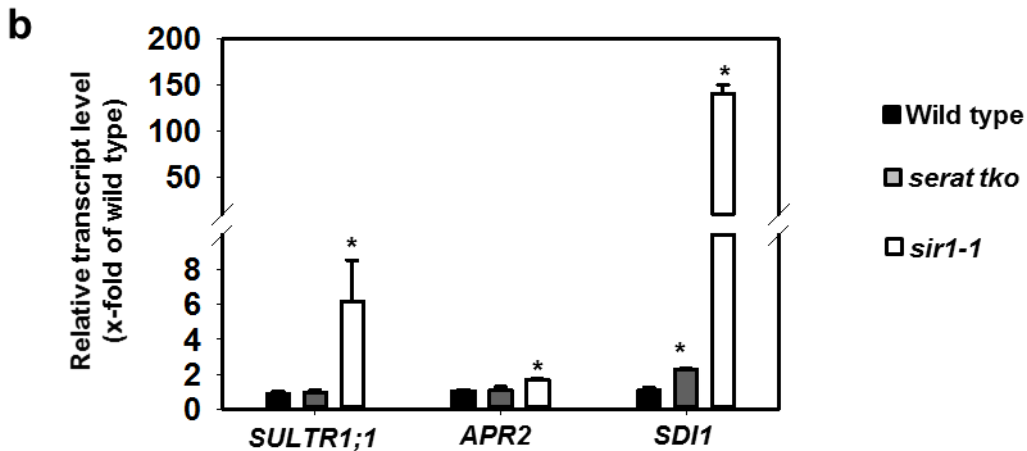
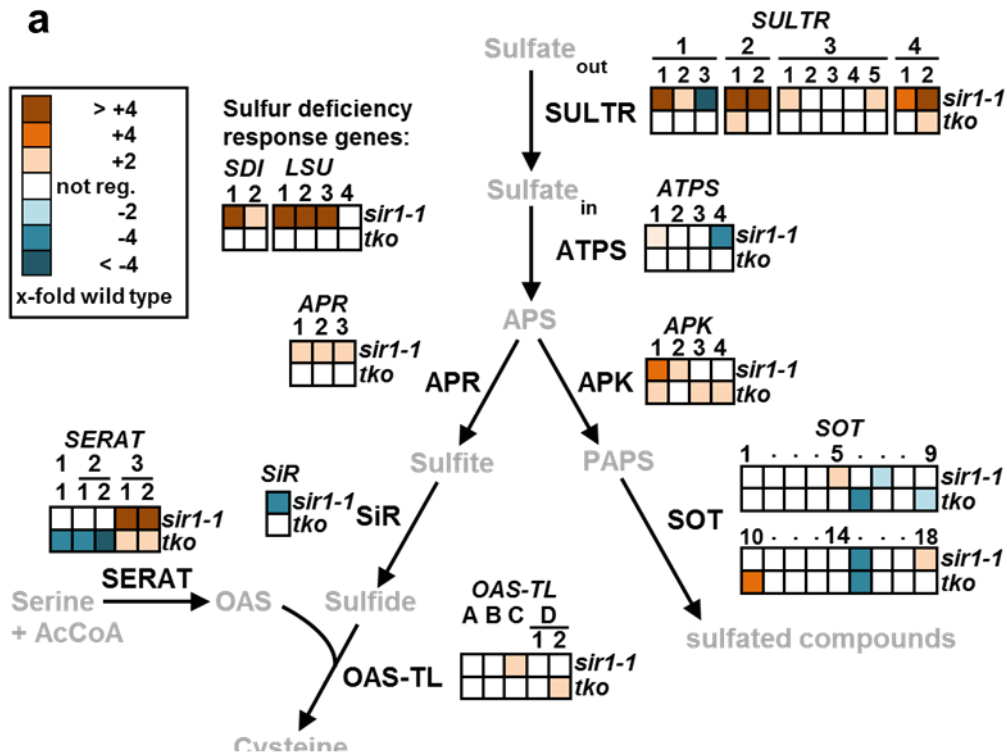
1



Supplementary Fig. 1 Characterization of cysteine synthesis depleted mutants. (a) Genotyping of *serat tko* and *sir1-1* mutants. Primers used for amplification of wild type (Genomic) or mutant (T-DNA) allele of respective genes (Serat1;1, Serat2;1, Serat2;2 and SiR) are listed in Table S4. (b) SERAT activity and (c) SiR protein abundances were quantified in wild type, *serat tko* and *sir1-1*. SERAT activity was measured according to Heeg et al., 2008<sup>1</sup>. SiR protein abundance was determined by immunological detection (n=3, mean±s.e.m., one way ANOVA, \*, p<0.05). (d) Fresh weight of shoot and root from 7-week old wild type, *serat tko* and *sir1-1* grown hydroponically on ½ Hoagland

medium (n>20, mean±s.e.m., one way ANOVA, \*, p<0.05). (e) Principle component analysis of metabolite data from shoot and root of wild type, *serat tko* and *sir1-1* (n=3). (f) Energy charge was calculated from absolute ATP, ADP and AMP concentrations. Energy charge=(ATP+0.5\*ADP)/(ATP+ADP+AMP) (n=3, mean±s.e.m., one way ANOVA, \*, p<0.05).

Supplementary Fig.

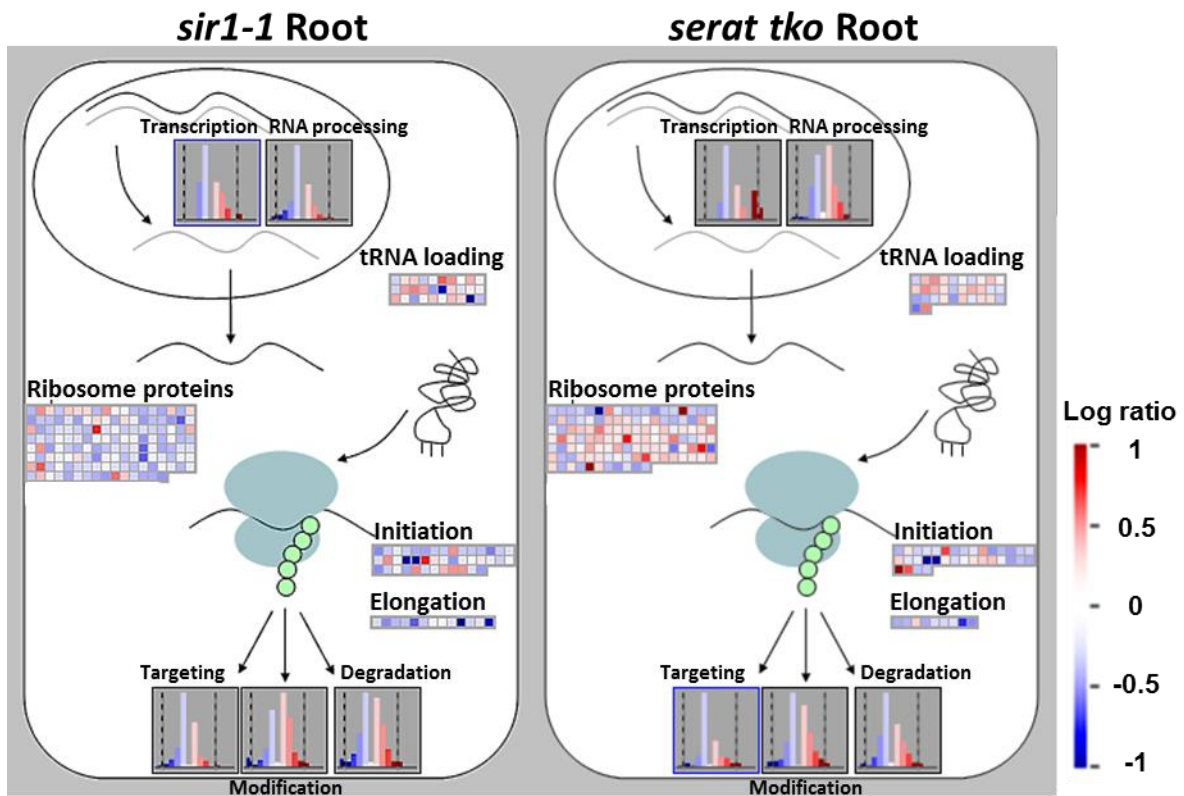


2

Supplementary Fig. 2 Specific up-regulation of sulfate uptake and assimilation in *sir1-1* mutant. (a) Transcript levels of genes (italics) that catalyze single step reactions (continuous arrows) are indicated by color code. White color represents no significant change ( $p < 0.05$ ,  $> 1.25$  fold change,  $n = 3$ ). (b) Transcriptional induction of selected genes within the sulfur assimilation pathway was confirmed by q-RT-PCR ( $n = 3$ ,  $\text{mean} \pm \text{s.e.m.}$ , one way ANOVA, \*,  $p < 0.05$ ). Primers used for q-RT-PCR are listed in Supplementary Table 4.

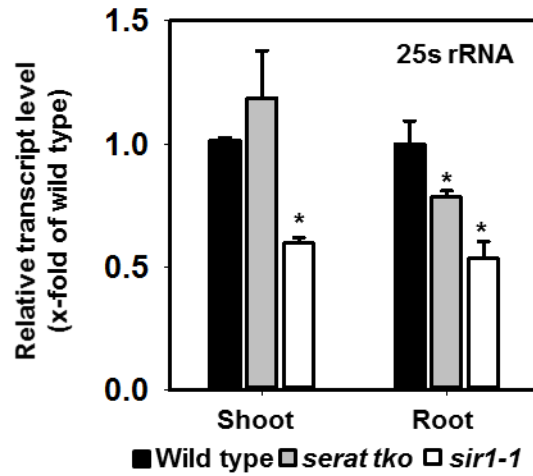


Supplementary Fig. 3



Supplementary Fig. 3 Specific transcriptional down-regulation of ribosome proteins in *sir1-1*. The entire protein biosynthesis pathway is presented and modified based on Mapman<sup>TM</sup>. The compared sets of genes contained transcripts which were identified by microarray analysis to be significantly up- or down regulated by more than 1.5-fold in *sir1-1* or *serat tko* in comparison to the wild type ( $n=3$ ,  $p<0.05$ ). A clear enrichment of down-regulated genes encoding for ribosome proteins and proteins involved in RNA processing is evident in the root of *sir1-1*. An increase of down-regulated genes is also observed in the category of RNA processing in *sir1-1* root. Please note that there are only significantly altered transcripts shown and hence no white squares appear in the graphic. However, light blue signals appear as white signal due to automatic settings of Mapman<sup>TM</sup> (<http://mapman.gabipd.org/>). Bar diagrams represents the frequency distribution of down-regulated genes in indicated process. Striped lines in the diagrams indicate +1 and -1 log ratio.

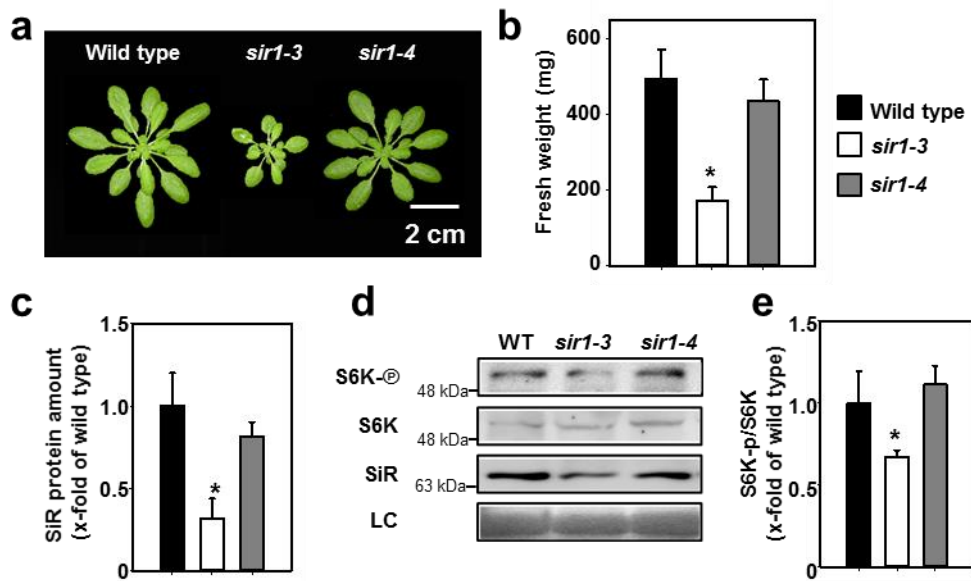
Supplementary Fig. 4



Supplementary Fig. 4 Transcript levels of 25s rRNA in cysteine synthesis depleted mutants.

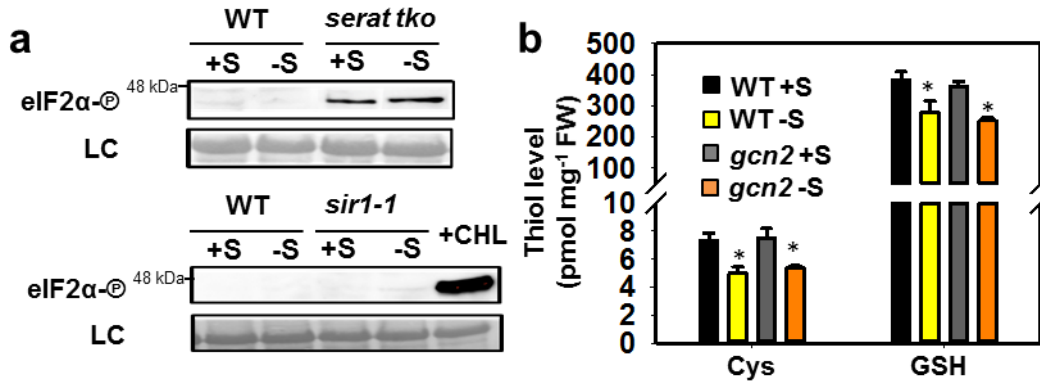
Total RNA was extracted from shoots and roots of 7-week old wild type (black), *serat tko* (grey) and *sir1-1* (white) grown hydroponically on ½ Hoagland medium. Relative transcript levels of 25s rRNA were determined according to Ren, Qiu<sup>3</sup>. Primers used for specific amplification of 25s rRNA are listed in Table S4. (n=3, mean±s.e.m., one way ANOVA, \*, p<0.05)

Supplementary Fig. 5



Supplementary Fig. 5 Limitation of SiR activity decreases TOR activity. (a) Shoot phenotype and (b) fresh weight of 5-week old wild type (black), *sir1-3* (white) and *sir1-4* (grey) grown on soil under short day conditions<sup>4</sup> (n=3, mean±s.e.m., one way ANOVA, \*, p<0.05). (c) SiR protein level in wild type, *sir1-3* and *sir1-4* was determined by immunological detection with a specific antiserum shown in d (n=3, mean±s.e.m., one way ANOVA, \*, p<0.05). (d) Immunological detection of S6K-p (52 kDa), S6K (52 kDa) and SiR (72 kDa) with specific antisera. Coomassie stained protein served as loading control (LC). TOR activity was determined by antibodies against S6K-p (52 kDa) and S6K (52 kDa) and (e) The ratio of S6K-p/S6K was calculated as a measure for *in vivo* TOR activity in the different mutants and displayed as x-fold of wild type level for easier comparison (n=3, mean±s.e.m., one way ANOVA, \*, p<0.05).

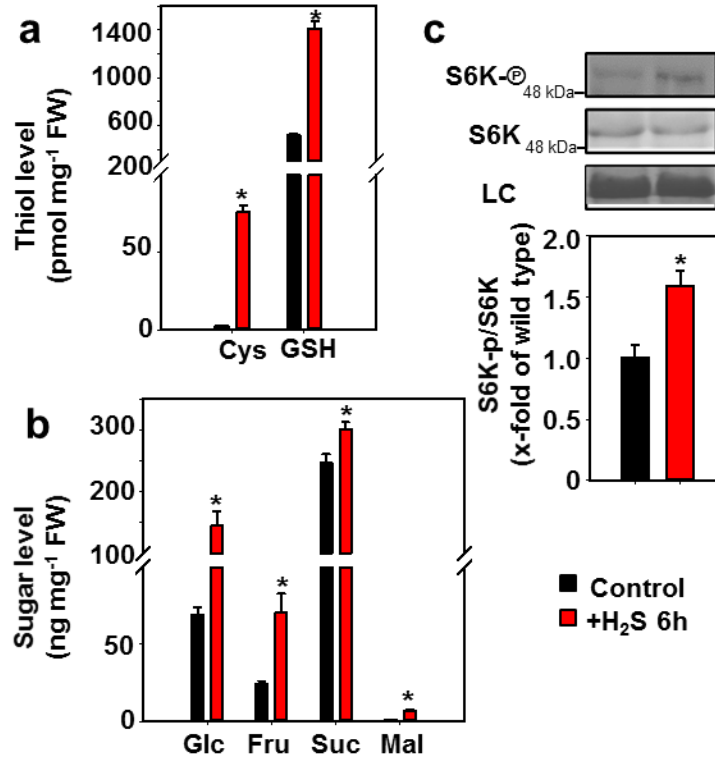
Supplementary Fig. 6



Supplementary Fig. 6 (a) GCN2 activity was determined by the level of eIF2α-p (apparent size: 43 kDa) in the shoot of wild type (WT), *serat tko* and *sir1-1* grown for 5 weeks under regular (+S, 500 mM sulfate) and restricted sulfur supply (-S, 1 mM sulfate). Application of chlorsulfuron (+CHL, 0.5 μM, 2h) to plants grown under regular nutrient supply served as positive control for phosphorylation of eIF2α, since CHL specifically induces GCN2 activity<sup>5</sup>. (b) Cysteine (Cys) and glutathione (GSH) were measured in WT and *gcn2* mutants grown under regular and sulfur deficient supply. 5-week old WT and *gcn2* mutants grown for 1 weeks under regular (+S, 500 mM sulfate) and restricted sulfur supply (-S, 0 mM sulfate) (n=4, mean±s.e.m., one way ANOVA, \*, p<0.05).

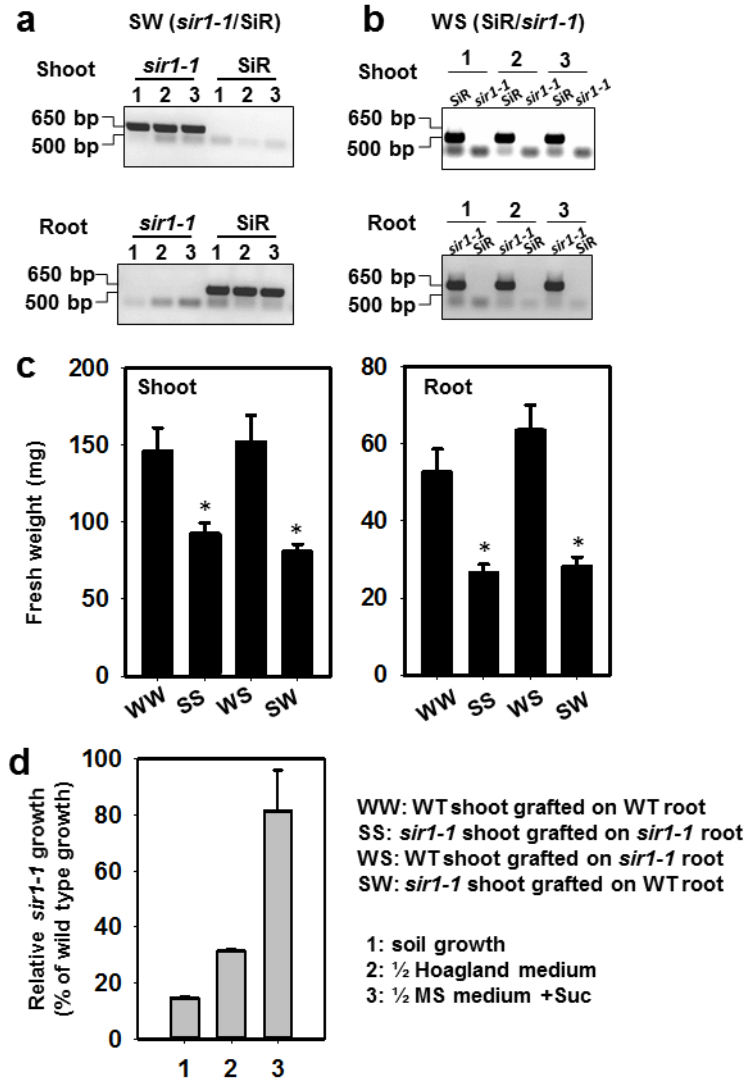


Supplementary Fig. 7



Supplementary Fig. 7 Short-term sulfide fumigation enhances soluble sugar levels and TOR activity in leaves of 5-week old wild type plants grown on soil in gas-controlled fumigation chambers. (a) Thiols and (b) soluble sugars were measured in the shoot of plants fumigated without (black, control) and with 1 ppm H<sub>2</sub>S for 6 hours (red, n=4, mean±s.e.m., t-test, \*, p<0.05). (c) Immunological detection of S6K-p (apparent size: 52 kDa) and S6K (apparent size: 52 kDa) with specific antisera in the shoot of 5-week old wild type plants fumigated without and with 1 p.p.m H<sub>2</sub>S for 6 hours. The ratio of S6K-p/S6K was calculated as a measure for the *in vivo* TOR activity. For easier comparison the *in vivo* TOR activity in non-fumigated plants was set to 1 (n=3, mean±s.e.m., t-test, \*, p<0.05).

Supplementary Fig. 8

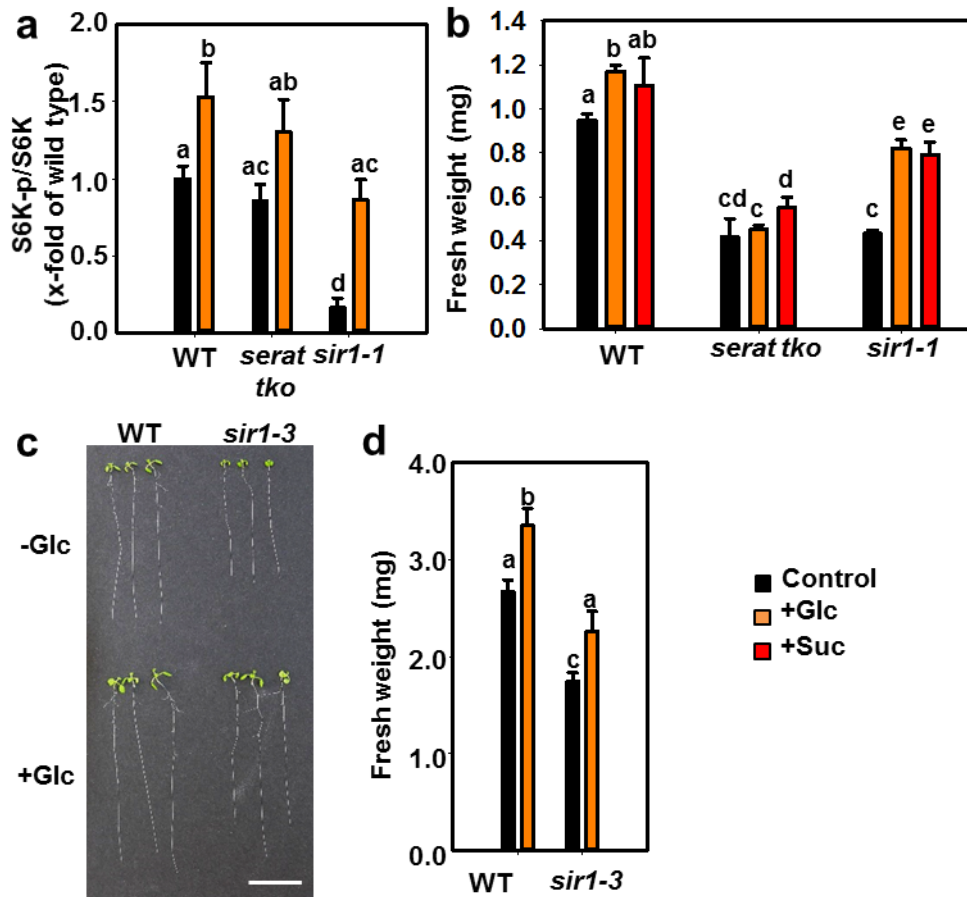


Supplementary Fig. 8 Characterization of chimeric *sir1-1*/wild type plants obtained by organ grafting.

(a-b) Confirmation of the correct genotype in shoots and roots of chimeric *sir1-1*/wild type plants. Primers used for genotyping are listed in supplementary table 4. (a) Organ-specific genotyping of *sir1-1* shoot grafted on WT root (SW). (b) Organ-specific genotyping of WT shoot grafted on *sir1-1* root (WS). (c) Fresh weight of shoot (left panel) and root (right panel) from 5-week old chimeric plants (WS and SW) grown on 1/s MS medium. WT shoot grafted on WT root (WW) and *sir1-1* shoot grafted on *sir1-1* root (SS) served as controls for the impact of grafting on growth. (n>20, mean±s.e.m., one

way ANOVA, \*,  $p < 0.05$ ) (d) Relative growth of *sir1-1* grown on different media. Shoot biomass of 5-week old wild type and *sir1-1* plants grown on soil (1), ½ Hoagland medium (2) or ½ MS-medium supplement with 1 % sucrose was determined ( $n=4$ ,  $\text{mean} \pm \text{s.e.m.}$ ). The relative growth of *sir1-1* (% of wild type) under the applied condition was calculated by division of *sir1-1* biomass with wild type biomass multiplied by 100% ( $(\textit{sir1-1} \text{ biomass} / \text{wild type biomass}) \times 100 \%$ ).

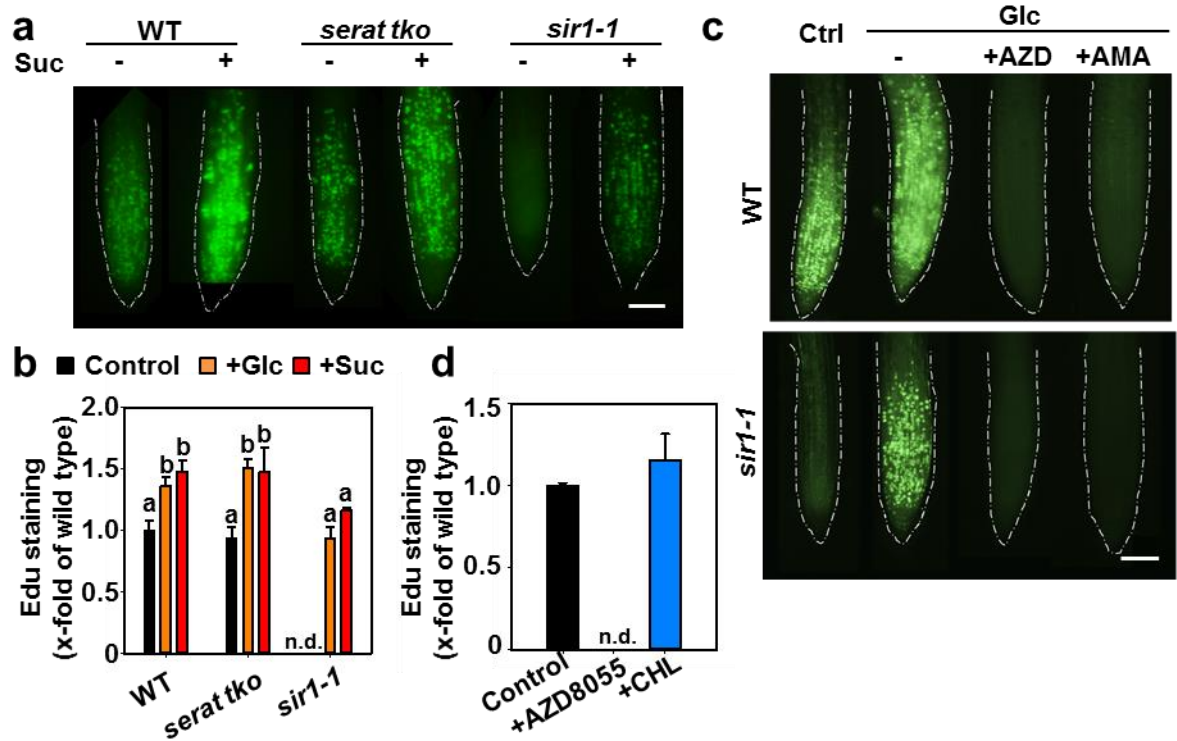
Supplementary Fig. 9



Supplementary Fig. 9 Decreased growth of the *serat* and *serat sir1-3* mutant was rescued by re-activation of glucose-TOR signaling. (a) Quantification of S6K-p/S6K signals shown in figure 4B as a proxy for the *in vivo* TOR activity in wild type and cysteine synthesis depleted mutants treated with (orange) or without (black) 30 mM glucose (n=4, mean±s.e.m., one way ANOVA, different letters indicating a significant difference, p<0.05). (b) Fresh weight of 7-day old wild type, *serat tko* and *serat tko sir1-1* grown on ½ MS-medium (black) supplemented with 30 mM glucose (+Glc, orange) or 15 mM sucrose (+Suc, red) was determined (n=4, mean±s.e.m., one way ANOVA, different letters indicating a significant difference, p<0.05). (c) Phenotype and (d) fresh weight of 10-day old wild type and *serat sir1-3* was determined in absence (-Glc, black) or presence of 30 mM glucose (+Glc, orange, n=4, mean±s.e.m., one way ANOVA, different letters indicating a significant difference, p<0.05).

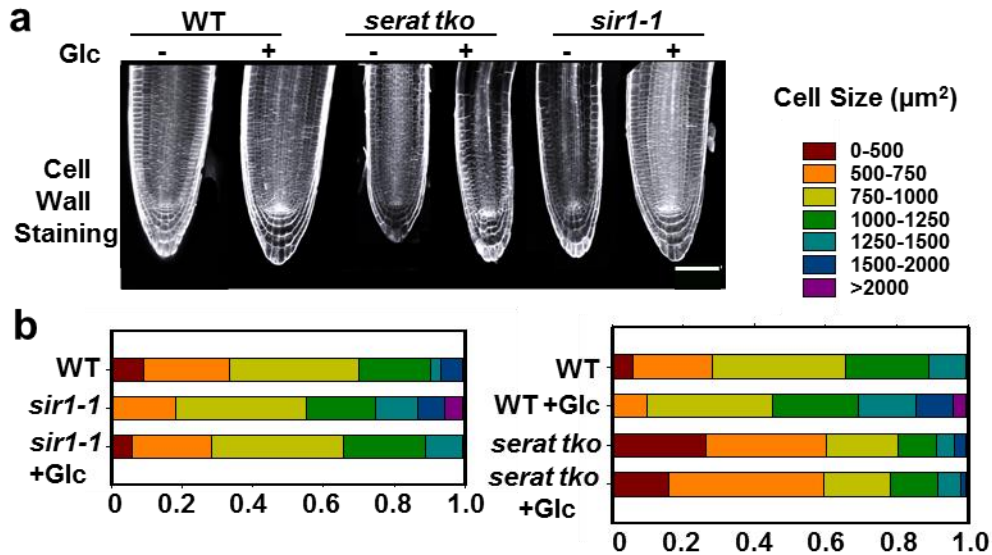


Supplementary Fig. 10



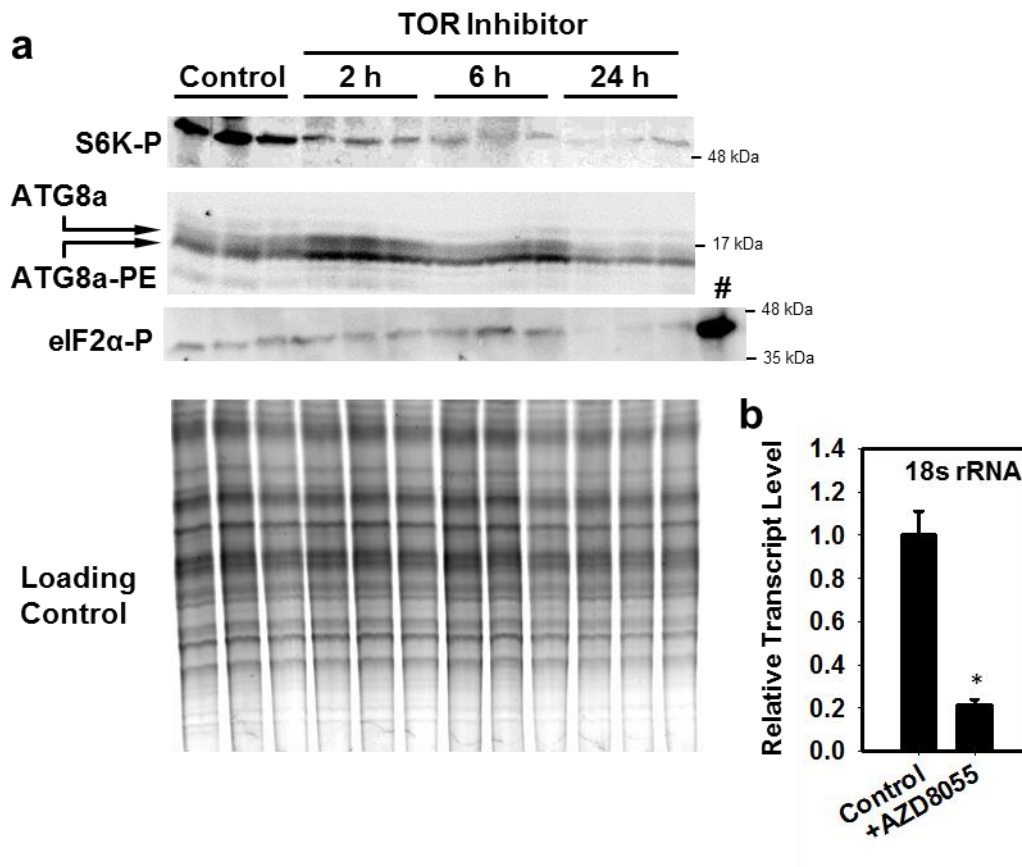
Supplementary Fig. 10 Root meristem activity specifically responds to S-precursor supply for cysteine biosynthesis via glucose-TOR signaling. (a) Root meristem activity was determined by Edu staining<sup>6</sup> in wild type and cysteine synthesis depleted mutants grown on AT medium in absence (-Suc) or presence of 15 mM sucrose (+Suc). Scale bar, 25  $\mu$ m. (b) Quantification of the fluorescent signal after 30 min of Edu staining shown in figure 4E and S11A. Signal intensity was shown in x-fold to the wild type under control condition (n=4-10, mean $\pm$ s.e.m., n.d., not detectable, one way ANOVA, different letters indicating a significant difference, p<0.05). Details of fluorescent imaging see supplemental methods (Edu staining). (c) Wild type and *sir1-1* were grown on AT medium (Ctrl) supplemented with 30 mM Glc for 7 days. Glc supplemented plants were treated for 2 hours with TOR inhibitor (AZD8055, 5  $\mu$ M) or antimycin A (AMA, 1  $\mu$ M), an inhibitor of mitochondrial respiration due to binding to the Qi site of cytochrome c reductase. Root meristem activity was determined by Edu staining. Scale bar, 25  $\mu$ m. (d) Quantification of the fluorescent signal from Edu staining shown in figure 4F (+AZD8055: application of selective TOR inhibitor, +CHL: chlorsulfuron application for specific activation of GCN2). Signal intensity was shown in x-fold to the wild type under control condition (n=4-10, mean $\pm$ s.e.m., n.d., not detectable, p<0.05).

Supplementary Fig. 11



Supplementary Fig. 11 Cell size at the root meristem in cysteine synthesis depleted mutants. (a) Cell size at the root meristematic zone was visualized and measured by cell wall staining. Cell wall was stained with 0.1 % SR 2200 solution. Scale bar, 25  $\mu\text{m}$ . (b) Distribution of the cell sizes at the root meristematic zone. Cell size was measured from the cell wall staining shown in A along single epidermal cell files. The meristematic zone was defined as the region of isodiametric cells from the QC up to the cell that was twice the length of the immediately preceding cell <sup>7</sup>. The size of epidermal cells was determined by CellSet <sup>8</sup> (n>10).

Supplementary Fig. 12

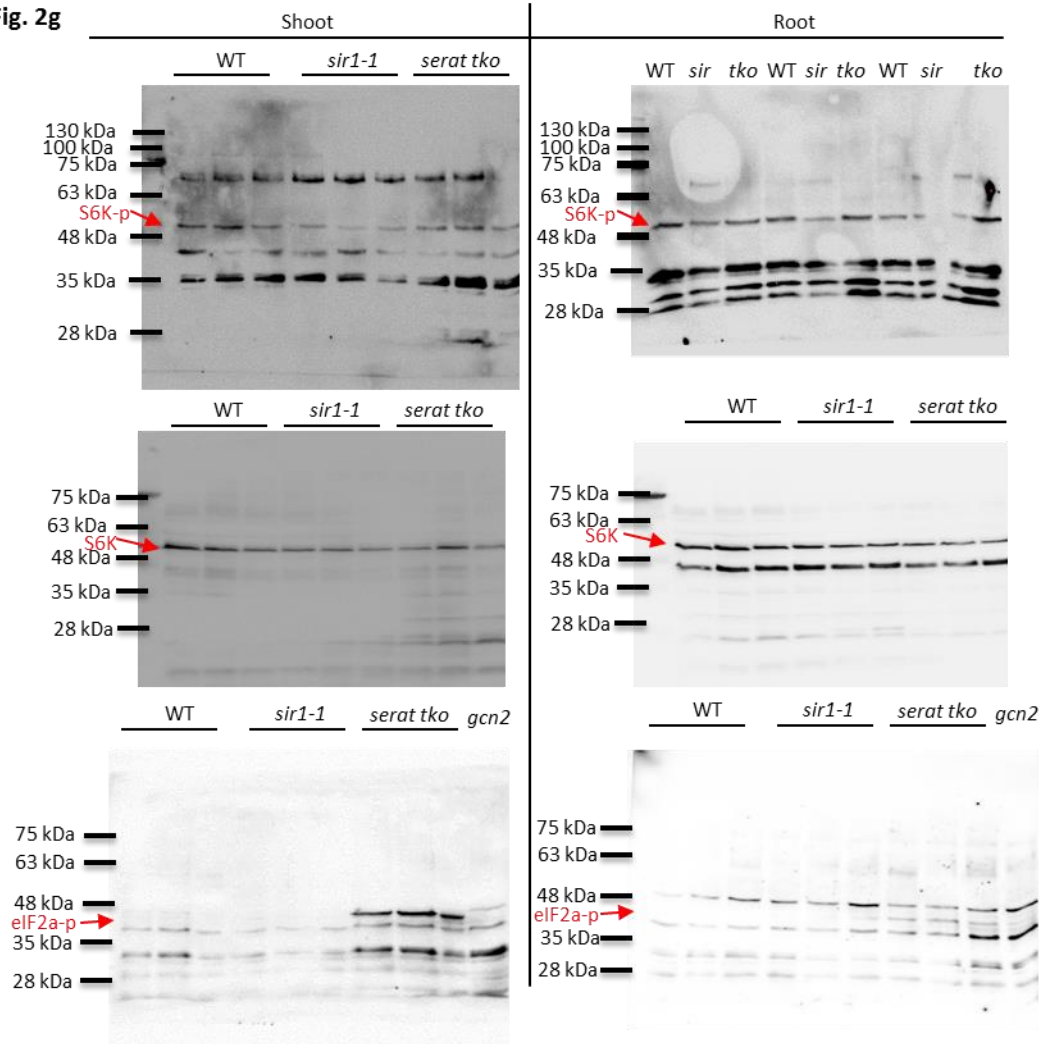


Supplementary Fig. 12 (a) TOR activity, autophagy induction and GCN2 activity were detected by antibodies against S6K-p (apparent size: 52 kDa), ATG8a (apparent size: 15-20 kDa) and eIF2 $\alpha$ -p (apparent size: 43 kDa) in roots of 7-week old WT plants grown in hydroponic medium after 2h, 6h and 24h treatment with 5  $\mu$ M TOR inhibitor AZD8055. Chlorsulfuron treatment (+CHL, 0.5  $\mu$ M, 2h) was used as a positive control for GCN2 activity (#). Total root protein was stained with Coomassie as loading control. Please note that equal sample volume (20  $\mu$ l) extracted from 50 mg of plant material were loaded. (b) 18s rRNA level was measured by qRT-PCR after 6 h AZD8055 treatment (n=3, mean $\pm$ s.e.m., t-test, \*, p<0.05). The inhibition of TOR for more than 6 hours decreased total extractable protein level, which is well explainable by the combination of decreased translation and enhanced autophagy. This decrease contributed to the lower signal for eIF2 $\alpha$ -P after 24 hours of AZD8055 treatment.

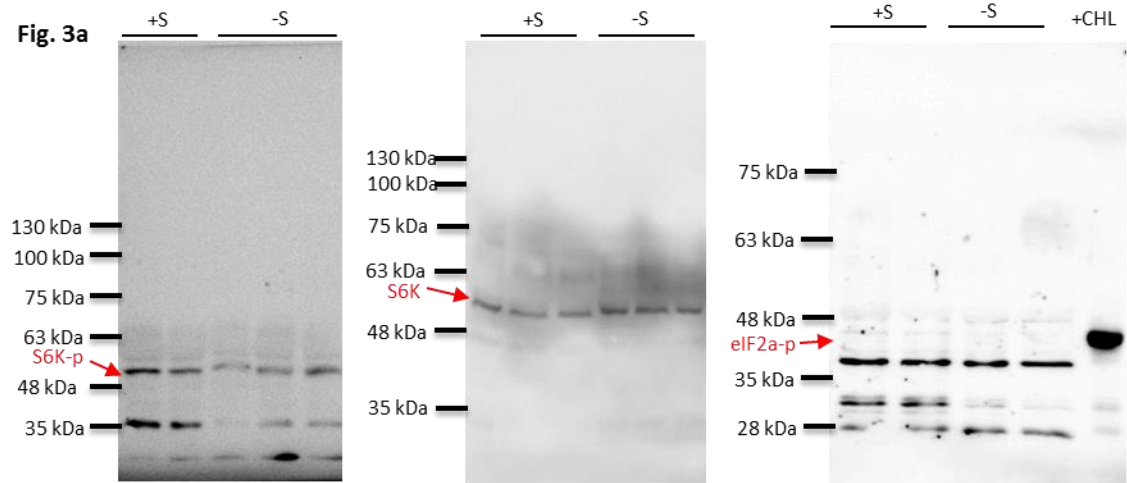


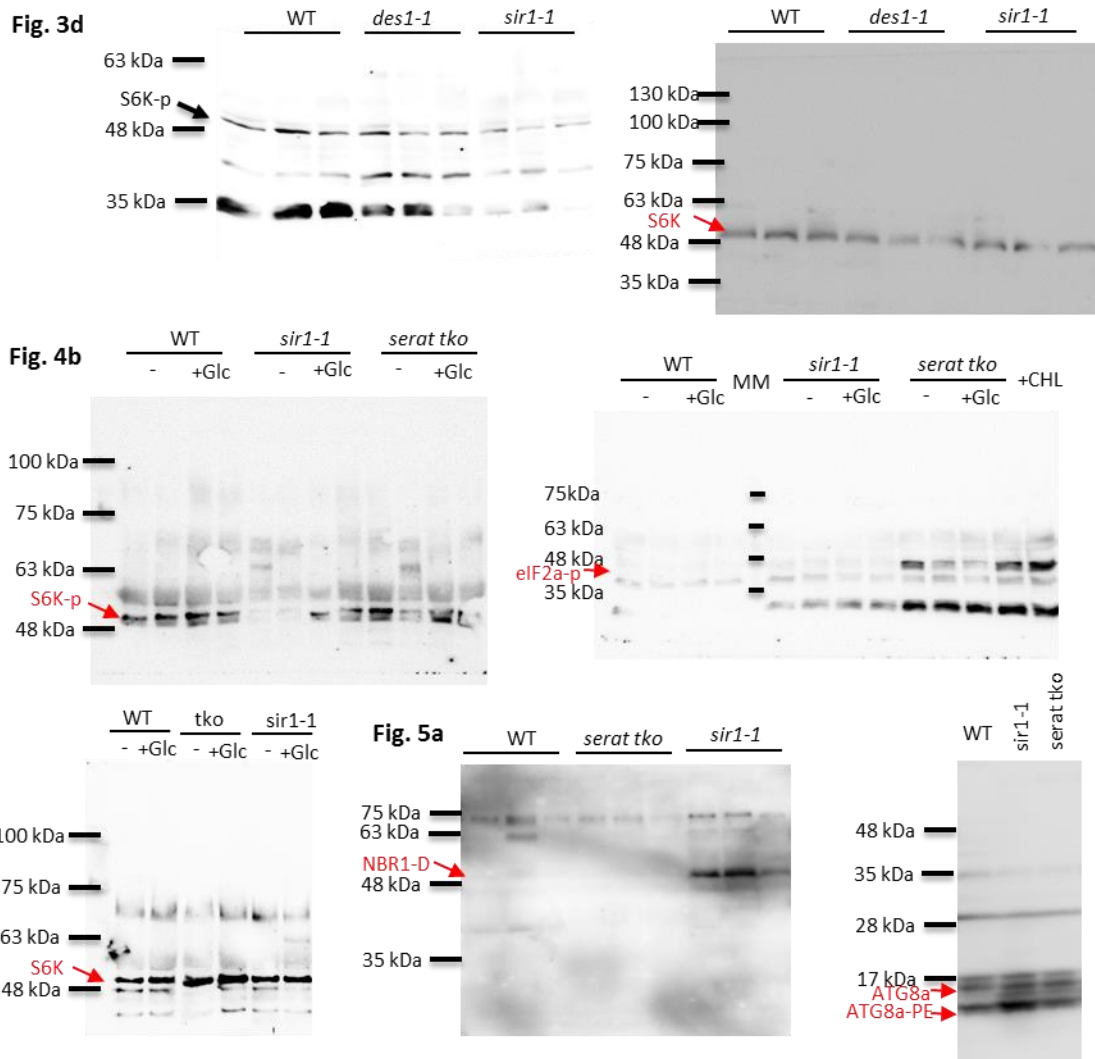
Supplementary Fig. 13

**Fig. 2g**



**Fig. 3a**





Supplementary Fig. 13 Uncropped Western blots related to Figure 2, 3, 4 and 5.

Supplementary Tables:

**Supplementary Table 1: Functional categories down-regulated in *sir1-1* root**

Functional category analysis by DAVID<sup>9</sup> of down-regulated transcripts in roots of 7-week-old cysteine synthesis depleted mutants that were grown hydroponically under short day conditions (fold change: 1.25,  $p < 0.05$ , FDR < 25%). FDR, false discovery rate

<b>Down-regulated transcripts in <i>sir1-1</i> root</b>			
<b>Term</b>	<b>PValue</b>	<b>Fold Enrichment FDR</b>	
ath00280:Valine, leucine and isoleucine degradation	8.07E-05	3.301587	0.091729
ath03008:Ribosome biogenesis in eukaryotes	8.89E-04	2.157473	1.006782
ath04141:Protein processing in endoplasmic reticulum	0.001861	1.673407	2.095735
ath01110:Biosynthesis of secondary metabolites	0.003159	1.23464	3.533886
ath01130:Biosynthesis of antibiotics	0.003446	1.408578	3.849426
ath01200:Carbon metabolism	0.004264	1.549982	4.743826
ath00010:Glycolysis / Gluconeogenesis	0.008256	1.840708	8.997696
<b>Down-regulated transcripts in <i>serat tko</i> root</b>			
<b>Term</b>	<b>PValue</b>	<b>Fold Enrichment FDR</b>	
ath00500:Starch and sucrose metabolism	2.10E-04	2.419494	0.237781
ath00280:Valine, leucine and isoleucine degradation	0.001138	3.360409	1.285014
ath00250:Alanine, aspartate and glutamate metabolism	0.00192	3.150383	2.158526
ath04141:Protein processing in endoplasmic reticulum	0.004096	1.757623	4.553103

**Supplementary Table 2: Functional categories up-regulated in *sir1-1* root**

Functional category analysis by DAVID<sup>9</sup> of up-regulated transcripts in roots of 7-week-old cysteine synthesis depleted mutants that were grown hydroponically under short day conditions (fold change: 1.25,  $p < 0.05$ ,  $FDR < 25\%$ ). FDR, false discovery rate

<b>Up-regulated transcripts in <i>sir1-1</i> root</b>			
<b>Term</b>	<b>PValue</b>	<b>Fold Enrichment FDR</b>	
ath00920:Sulfur metabolism	7.97E-08	4.497415	9.16E-05
ath00260:Glycine, serine and threonine metabolism	9.96E-06	2.987866	0.011449
ath00270:Cysteine and methionine metabolism	5.27E-05	2.483421	0.060546
ath00511:Other glycan degradation	1.38E-04	5.122056	0.15897
ath00531:Glycosaminoglycan degradation	1.53E-04	8.780667	0.175497
ath01230:Biosynthesis of amino acids	7.26E-04	1.687265	0.831961
ath00950:Isoquinoline alkaloid biosynthesis	9.99E-04	4.008565	1.142721
ath00350:Tyrosine metabolism	0.001121	3.073233	1.281685
ath01210:2-Oxocarboxylic acid metabolism	0.001642	2.353377	1.872081
ath00960:Tropane, piperidine and pyridine alkaloid biosynthesis	0.001724	3.130145	1.964665
ath00903:Limonene and pinene degradation	0.003684	2.430806	4.154825
ath00500:Starch and sucrose metabolism	0.004107	1.884916	4.621143
ath00604:Glycosphingolipid biosynthesis - ganglio series	0.007906	8.195289	8.720867
ath04146:Peroxisome	0.00884	2.001723	9.704279
<b>Up-regulated transcripts in <i>serat tko</i> root</b>			
<b>Term</b>	<b>PValue</b>	<b>Fold Enrichment FDR</b>	
ath03030:DNA replication	4.41E-04	3.230753	0.500724
ath00561:Glycerolipid metabolism	6.48E-04	3.106494	0.733984
ath00910:Nitrogen metabolism	0.001406	3.254422	1.587012
ath00062:Fatty acid elongation	0.005469	3.19525	6.046287
ath04626:Plant-pathogen interaction	0.007677	1.797468	8.391184
ath00564:Glycerophospholipid metabolism	0.007873	2.167321	8.597136

**Supplementary Table 3: Functional categories down-regulated in plants with decreased sulfur assimilation either by impaired SiR activity in *sir1-1* or limited sulfate supply of wild type**

Functional category analysis by DAVID<sup>9</sup> of down-regulated transcripts in roots of 7-week-old plants that were grown hydroponically under short day conditions (fold change: 1.25,  $p < 0.05$ ,  $FDR < 25\%$ ). FDR, false discovery rate. The *sir1-1* plants were grown in sulfate containing medium and compared to wild type plants grown under the same conditions. Limited sulfate supply for wild type plants was achieved by decreasing sulfate concentration in the medium from 500  $\mu\text{M}$  to 1  $\mu\text{M}$ .

<b>Down-regulated transcripts in <i>sir1-1</i> shoot</b>			
<b>Term</b>	<b>PValue</b>	<b>Fold Enrichment FDR</b>	
ath00945:Stilbenoid, diarylheptanoid and gingerol biosynthesis	4.30E-04	2.733389	0.47208
ath00903:Limonene and pinene degradation	7.14E-04	2.614546	0.782247
ath00710:Carbon fixation in photosynthetic organisms	0.004892	2.255046	5.247321
ath04144:Endocytosis	0.00981	2.255046	10.26968
ath00520:Amino sugar and nucleotide sugar metabolism	0.009916	2.162373	10.37585
ath00051:Fructose and mannose metabolism	0.014606	2.505607	14.93338
ath01064:Biosynthesis of alkaloids derived from ornithine, lysine and nicotinic acid	0.031144	1.562231	19.37443
ath00010:Glycolysis / Gluconeogenesis	0.035758	1.835502	22.98479
ath04070:Phosphatidylinositol signaling system	0.039546	2.437887	24.82238
<b>Down-regulated transcripts in WT shoot under sulfur deficiency</b>			
<b>Term</b>	<b>PValue</b>	<b>Fold Enrichment FDR</b>	
ath00196:Photosynthesis	2.31E-07	4.236957	2.58E-04
ath01062:Biosynthesis of terpenoids and steroids	1.58E-04	1.585017	0.176664
ath01070:Biosynthesis of plant hormones	4.08E-04	1.412319	0.456108
ath00906:Carotenoid biosynthesis	0.003398	2.683406	3.74118
ath00520:Amino sugar and nucleotide sugar metabolism	0.004934	1.764431	5.389783
ath00061:Fatty acid biosynthesis	0.005033	2.566736	5.495378
ath00710:Carbon fixation in photosynthetic organisms	0.007128	1.71738	7.700545
ath00010:Glycolysis / Gluconeogenesis	0.010777	1.622525	11.42986
ath01066:Biosynthesis of alkaloids derived from terpenoid and polyketide	0.013562	1.419608	14.18314
ath00500:Starch and sucrose metabolism	0.014583	1.585649	15.1723
ath01064:Biosynthesis of alkaloids derived from ornithine, lysine and nicotinic acid	0.02598	1.357868	15.53613
ath00910:Nitrogen metabolism	0.035922	1.788937	23.62022
ath00100:Steroid biosynthesis	0.038501	2.064159	23.58254

ath00030: Pentose phosphate pathway	0.03925	1.683706	24.14204
ath00620: Pyruvate metabolism	0.044838	1.56876	24.1812

**Supplementary Table 4: Primers used for qRT-PCR and genotyping**

<b>qRT-PCR primers</b>	
<b>18s rRNA_for</b>	GCAATTGTTGGTCTTCAACGAG
<b>18s rRNA_rev</b>	CAGGGACGTAGTCAACGCG
<b>18s rRNA_RT</b>	CAATGATCCTTCCGCAGGTTCA
<b>25s rRNA_for</b>	CGTCTTCGGCGTTCGAATTG
<b>25s rRNA_rev</b>	GGGCTCTCACCTCTCTG
<b>25s rRNA_RT</b>	TCGAATCTTAGCGACAAAGGGC
<b>SULTR1;1_for</b>	GCCATCACAATCGCTCTCAA
<b>SULTR1;1_rev</b>	TTGCCAATTCACCCATGC
<b>APR2_for</b>	GAGGAAGATGGTGCTGCAGAC
<b>APR2_rev</b>	CCTCCTTGCTCAATGCAACCAC
<b>SDI1_for</b>	GTGGAGACACTCCTTATGTCAGAGC
<b>SDI1_rev</b>	CTCTGTCTCCAGTGTTGATGGC
<b>TIP41_like_for</b>	GATGAGGCACCAACTGTTCTTCGTG
<b>TIP41_like_rev</b>	CTGACTGATGGAGCTCGGGTCG
<b>Genotyping primers</b>	
<b>serat1.1_LP</b>	AGTCTCGCCGGATTCCCAACCG
<b>serat1.1_RP</b>	GCTGCTGCAACAGAAGGGATGC
<b>serat2.1_LP</b>	AGGGCGACTGCTTCACGTAAC
<b>serat2.1_RP</b>	CACCAATCAACCTCGCCGGATT
<b>serat2;2_LP</b>	GGTCACAAGTCGCCGCACTTC
<b>serat2;2_RP</b>	CCGTCTCACCGATCACAATAGCCG
<b>sir1-1_RP</b>	GCCCAACACAACACTTACACC
<b>sir1-1_LP</b>	GGAGCTCGAAACGTGATGACATCG

## Supplementary Methods

**Plant Growth Conditions** Sucrose/glucose feeding experiment were performed with seedlings grown on AT medium (pH5.8, 0.6% Agar) supplemented with 30 mM glucose or 15 mM sucrose. Glc supplemented plants were treated for 2 hours with TOR inhibitor (AZD8055, 5  $\mu$ M) or antimycin A (AMA, 1  $\mu$ M), an inhibitor of mitochondrial respiration due to binding to the Qi site of cytochrome c reductase.

For sulfide fumigation experiment, wild type plants were grown on soil for 5 weeks and then fumigated with 1 ppm H<sub>2</sub>S for 6 hours.

All plants were grown in a short-day climate chamber (8.5 h light/15.5 h dark; 80-100  $\mu$ mol m<sup>-2</sup>s<sup>-1</sup>; 22°C day/18°C night; 50% humidity).

**Genomic Characterization** Genomic DNA from leaf or root material was isolated as outlined in Edwards, Johnstone<sup>10</sup>. For genomic characterization of homozygous plants, PCR was performed according to GLP standards, with the isolated gDNA and specific primer pair combinations outlined in Supplementary Table 4.

**Determination of SERAT Enzyme Activity** SERAT activity in leaves was determined as described in Heeg et al., 2008, with the only difference that 2 units purified recombinant OAS-TL<sup>11</sup> was used to achieve the abundance of OAS-TL activity. The assay was performed in a total volume of 100  $\mu$ l containing 58  $\mu$ l protein extract from 100 mg plant material, 50 mM HEPES/KOH pH 7.5, 10 mM Na<sub>2</sub>S, 5 mM DTT, 10 mM serine and 2 unites OASTL. The reaction mix was incubated at 25°C for 5 min. Then 1 mM acetyl-coA was added and incubated at 25 °C for 30 min. The reaction was stopped by addition of 50  $\mu$ l 20% TCA. After centrifugation, the supernatant was transferred quantitatively to 200  $\mu$ l ninhydrin and 100  $\mu$ l acetic acid and boiled at 100°C for 10 min. Then samples were cooled down and mixed with 550  $\mu$ l 100% ethonal. The derivatives of ninhydrin-cysteine was measured at 560 nm with the photometer UvikonXL.

**Total RNA extraction** RNA was extracted from 50 mg of plant materials using the peqGOLD total RNA kit (peqLAB, Erlangen). The manufacturer's protocol was slightly modified to optimize the extraction. Briefly plant material was homogenized in 400  $\mu$ l lysis buffer T. DNase digestion was performed on the RNA binding column for 15 min at room temperature. RNA was eluted by 50  $\mu$ l RNase free water. RNA concentration was determined by Nanodrop.

**cDNA synthesis** RNA was converted to cDNA using cDNA synthesis kit (Fermentas), according to the manufacturer's protocol with 0.5  $\mu$ g RNA and 0.5  $\mu$ l oligo dT primers (for *SULTRI;1*, *APR2* and *SDII* detection) or 25s RNA\_RT primer (Supplementary Table 4, for 25s rRNA detection). RNA was incubated with oligo dT at 65°C for 5 min. Then cDNA synthesis was carried out at 42°C for 1 hour. The synthesized cDNA for mRNA detection was diluted 1:5 for qPCR. The synthesized cDNA for 25s rRNA detection was diluted 1:10000 for qPCR. 25s rRNA was measured according to Ren et al., 2011<sup>3</sup>.



**qRT-PCR** qRT-PCR was performed using the SYBR mix (qPCRBIO SyGreen Mix Lo-ROX) in the RotorQ cycler. Relative expression data was normalized against the expression of the reference gene TIP41-like (primers listed in Supplementary Table 4).

**Edu staining** 7-day old seedlings grown on AT medium (pH5.8, 0.6% Agar) supplemented with 30 mM Glc were transferred to AT medium supplemented with 30 mM Glc and 5  $\mu$ M AZD8055 (TOR inhibitor) or 5  $\mu$ M AMA (Mitochondria inhibitor) for 90 min. Then 5  $\mu$ l 1 $\mu$ M EdU in liquid AT medium was added directly on the root tip. The root tips were incubated with EdU for 30 min in the climate chamber. Then the seedlings were fixed in 100  $\mu$ l Fixation/Permeabilization reagent (4% Formaldehyde, 0.1% Triton X-100 in 1x PBS) for 30 min. After fixation, seedlings were incubated in the dark with 100  $\mu$ l Click-iT reaction cocktail (prepared according to the manufacturer's protocol, Click-iT® EdU Alexa Fluor® 488 Imaging Kit, Invitrogen). The seedling were washed with PBS buffer for 2 times and analysed by Leica DM IRB epifluorescent microscope with FITC/GFP filter (AlexaFluor 488: excitation 495 nm; emission 519 nm). Images were recorded by Leica DFC350 FX camera.

**Metabolites measurement** Thiol metabolites were extracted with 0.1 M HCL and separated on a LiChroCART 125x4 mm LiChrospher 60 RP-select column and quantified with the fluorescent dye monobromobimane (Synchem) described by <sup>12</sup>. Soluble sugars were extracted by 80% ethanol and separated on Dionex ICS-3000 system with CarboPac PA1 with CarboPac PA1-Guard column at 25°C.

**Immunological Detection of Proteins** Total soluble proteins were extracted from 50 mg plant materials with 250  $\mu$ l 2x Laemmli buffer supplemented with 1% phosphatase inhibitor cocktail 2 (Sigma). Proteins were denatured for 5 min at 95°C and separated on 10% SDS-PAGE. Subsequently, proteins were blotted to nitrocellulose membrane. The primary antibodies anti-S6k-p (Phospho-p70 S6 Kinase (p-Thr389), cell signaling, #9205, 1:5000), eIF-2 $\alpha$  Phospho (Epitomics, #1090-1, 1:10,000) and anti-SiR (Khan et al., 2010,1:5000) were detected using the HRP-conjugated secondary antibody (1:30,000). The band intensity was quantified by Image Quant LAS4000 version 1.21 and normalized by the loading control.

For autophagy detection by protein markers and detection of S6K, proteins were extracted from 50 mg materials in 100  $\mu$ l urea buffer (4 M urea, 100 mM DTT and 1% Triton X-100) and separated on 15% SDS PAGE containing 8 M urea. After separation, proteins were transferred to PVDF membrane. Antibodies against ATG8a-PE (1:2000) and NBR1 (1:5000) were described in <sup>13</sup>.

**Pinciple Component Analysis** The PCA of metabolites data was performed by MetaboAnalyst 3.0. Data was normalized to WT and log-transformed. Data scale was auto-scaled <sup>14</sup>.

**Cell size measurement** Cell wall was stained by 0.1 % SR 2200 solution (0.1% SR 2200, 1% DMSO, 0.05% Triton-X100, 5 % glycerol, 4 % paraformaldehyde) and immediately analyzed under a confocal scanhead LSM 510 META mounted on an Axiovert 200M

microscope. Cell size was measured from the cell wall staining along single epidermal cell files. The meristematic zone was defined as the region of isodiametric cells from the QC up to the cell that was twice the length of the immediately preceding cell<sup>7</sup>. Cell size was measured by the online-software CellSet (CPIB)<sup>8</sup>.

## Supplementary References

1. Heeg C, *et al.* Analysis of the *Arabidopsis* O-acetylserine(thiol)lyase gene family demonstrates compartment-specific differences in the regulation of cysteine synthesis. *Plant Cell* **20**, 168-185 (2008).
2. Khan MS, *et al.* Sulfite reductase defines a newly discovered bottleneck for assimilatory sulfate reduction and is essential for growth and development in *Arabidopsis thaliana*. *Plant Cell* **22**, 1216-1231 (2010).
3. Ren MZ, *et al.* Target of rapamycin regulates development and ribosomal RNA expression through kinase domain in *Arabidopsis*. *Plant Physiol.* **155**, 1367-1382 (2011).
4. Yarmolinsky D, Brychkova G, Fluhr R, Sagi M. Sulfite reductase protects plants against sulfite toxicity. *Plant Physiol.* **161**, 725-743 (2013).
5. Lageix S, *et al.* Arabidopsis eIF2alpha kinase GCN2 is essential for growth in stress conditions and is activated by wounding. *BMC Plant Biol.* **8**, 134 (2008).
6. Salic A, Mitchison TJ. A chemical method for fast and sensitive detection of DNA synthesis in vivo. *Proc. Natl. Acad. Sci. USA* **105**, 2415-2420 (2008).
7. Gonzalez-Garcia MP, *et al.* Brassinosteroids control meristem size by promoting cell cycle progression in *Arabidopsis* roots. *Development* **138**, 849-859 (2011).
8. Pound MP, French AP, Wells DM, Bennett MJ, Pridmore TP. CellSeT: Novel software to extract and analyze structured networks of plant cells from confocal images. *The Plant Cell* **24**, 1353-1361 (2012).
9. Huang DW, Sherman BT, Lempicki RA. Systematic and integrative analysis of large gene lists using DAVID bioinformatics resources. *Nat. Protoc.* **4**, 44-57 (2009).
10. Edwards K, Johnstone C, Thompson C. A simple and rapid method for the preparation of plant genomic DNA for PCR analysis. *Nucleic Acids Res.* **19**, 1349 (1991).
11. Wirtz M, Droux M, Hell R. O-acetylserine (thiol) lyase: an enigmatic enzyme of plant cysteine biosynthesis revisited in *Arabidopsis thaliana*. *J. Exp. Bot.* **55**, 1785-1798 (2004).
12. Forieri I, *et al.* System analysis of metabolism and the transcriptome in *Arabidopsis thaliana* roots reveals differential co-regulation upon iron, sulfur and potassium deficiency. *Plant Cell Environ.* **40**, 95-107 (2017).
13. Munch D, Rodriguez E, Bressendorff S, Park OK, Hofius D, Petersen M. Autophagy deficiency leads to accumulation of ubiquitinated proteins, ER stress, and cell death in *Arabidopsis*. *Autophagy* **10**, 1579-1587 (2014).
14. Xia JG, Sinelnikov IV, Han B, Wishart DS. MetaboAnalyst 3.0-making metabolomics more meaningful. *Nucleic Acids Res.* **43**, W251-W257 (2015).
15. Huang DW, Sherman BT, Lempicki RA. Bioinformatics enrichment tools: paths toward the comprehensive functional analysis of large gene lists. *Nucleic Acids Res.* **37**, 1-13 (2009).